WARWICK
THE UNIVERSITY OF WARWICK

Manuscript version: Author's Accepted Manuscript
The version presented in WRAP is the author's accepted manuscript and may differ from the published version or Version of Record.

Persistent WRAP URL:
http://wrap.warwick.ac.uk/175371

How to cite:
Please refer to published version for the most recent bibliographic citation information. If a published version is known of, the repository item page linked to above, will contain details on accessing it.

Copyright and reuse:
The Warwick Research Archive Portal (WRAP) makes this work by researchers of the University of Warwick available open access under the following conditions.

Copyright © and all moral rights to the version of the paper presented here belong to the individual author(s) and/or other copyright owners. To the extent reasonable and practicable the material made available in WRAP has been checked for eligibility before being made available.

Copies of full items can be used for personal research or study, educational, or not-for-profit purposes without prior permission or charge. Provided that the authors, title and full bibliographic details are credited, a hyperlink and/or URL is given for the original metadata page and the content is not changed in any way.

Publisher's statement:
Please refer to the repository item page, publisher's statement section, for further information.

For more information, please contact the WRAP Team at: wrap@warwick.ac.uk.

warwick.ac.uk/lib-publications

Enantioselective degrader for elimination of extracellular aggregation-prone proteins hIAPP associated with type 2 diabetes

Zhenqi Liu,[†,‡] Dongqin Yu,[†,‡] Hualong Song,[§] Miles Lewis Postings,[§] Peter Scott,[§] Zhao Wang,[†,‡] Jinsong Ren,[†,‡] and Xiaogang Qu[,†,‡]*

[†]Laboratory of Chemical Biology and State Key Laboratory of Rare Earth Resource Utilization, Changchun Institute of Applied Chemistry, Chinese Academy of Sciences, Changchun, Jilin 130022, P. R. China

[‡]School of Applied Chemistry and Engineering, University of Science and Technology of China, Hefei, Anhui 230026, P. R. China

[§]Department of Chemistry, University of Warwick, Coventry CV4 7AL, UK.

ABSTRACT: Targeted protein degradation (TPD) has been demonstrated powerful to modulate protein homeostasis. For overcoming the limitation to intracellular protein degradation, Lysosome targeting chimeras (LYTACs) have been recently developed and successfully utilized to degrade a range of disease-relevant extracellular and membrane proteins. Inspired by this strategy, here we describe our proof-of-concept studies using metallohelix-based degraders to deliver the

extracellular human islet amyloid polypeptide (hIAPP) into the lysosomes for degradation. Our designed α-helical peptide mimics, metallohelix can bind and inhibit hIAPP aggregation, and the conjugated tri-GalNAc motif can target macrophage galactose-type lectin 1 (MGL1), yielding chimeric molecules that can both inhibit hIAPP aggregation and direct the bound hIAPP for lysosomal degradation in macrophages. Further studies demonstrate that the enhanced hIAPP clearance has been through the endo-lysosomal system and depends on MGL1-mediated endocytosis. Intriguingly, Λ enantiomers show even better efficiency in preventing hIAPP aggregation and promoting internalization and degradation of hIAPP than Δ enantiomers. Moreover, metallohelix-based degraders also faciltate the clearance of hIAPP through asialoglycoprotein receptor (ASGPR) in liver cells. Overall, our studies demonstrate that chiral-metallohelix can be employed for targeted degradation of extracellular misfolded proteins and possess enantioaelectivity.

KEYWORDS: targeted protein degradation, lysosome targeting chimeras, metallohelix, enantioselective, human islet amyloid polypeptide.

Targeted protein degradation (TPD) technology has recently emerged as a promising therapeutic strategy for directly depleting protein of interest (POI) by using chimera molecules to promote their degradation.[1-3] TPD technologies such as Proteolysis-Targeting Chimaeras (PROTACs)[4-7] and Macroautophagy Degradation Targeting Chimeras (MADTACS)[8-11] have been developed depletion of proteins that have generally been considered "undruggable".[12] However, these TPD strategies principally rely on intracellular protein degradation machinery, and are therefore limited to targeting intracellular proteins. In 2019, the Bertozzi group[13, 14] have overcome this limitation

by engaging the endosome/lysosome degradation pathway by using chimeric molecules "lysosome targeting chimera (LYTACs)." LYTACs form a ternary complex that captures the secreted and membrane protein through a polypeptide or antibody conjugated with ligands for the lysosome targeting receptors (LTRs) that localizes at the plasma membrane, and directs cargoes for lysosomal trafficking and degradation.[15] This approach has been successfully applied to degrade several disease-relevant extracellular and membrane proteins, including ApoE4, EGFR, CD71, and PD-L1. Similarly, the recently reported MoDE (molecular degraders of extracellular proteins),[16] AbTACs (antibody-tartgeting chimeras),[17] bispecific aptamer chimeras,[18] and GlueTAC (covalently engineered nanobody chimeras)[19] also offer attractive approaches for extracellular/membrane protein degradation. They establish brilliant strategies for directing extracellular or transmembrane target protein for lysosomal trafficking and degradation with a wide range of therapeutic applications.

The extracellular protein aggregates are linked to more than 30 devasting degenerative diseases, including type 2 diabetes (T2D), Alzheimer's disease (AD), and many other amyloidoses.[20] Phagocytes maintain homeostasis in human body through phagocytic clearance of protein aggregates and cellular debris.[21] Unfortunately, this function deteriorates during ageing and neurodegenerative disease.[21-23] Inspired by TPD strategy, we envisioned that bifunctional molecules capable of binding both extracellular protein aggregates and cell-surface LTRs could transport target into lysosomes for further degradation, offering an approach to accelerate the clearance of misfolded proteins. However, misfolded proteins in amyloidosis are generally regarded as "undruggable" because it lacks potential binding sites for small molecules to bind.[24, 25] The immunogenicity and stability of antibodies or polypeptide remains to be solved.[26] In addition, cleavage sites of amyloid proteins are usually embedded inside the β-sheet structures that

limit access by proteases, which cause the poor ability of lysosomes to degrade these protein aggregates.[22, 27] Therefore, a synthetic extracellular amyloid degradation platform with reduced immunogenicity, higher efficiency, and biocompatibility is highly desirable.

Chiral metallohelices, three-dimensional coordination complexes of three α-helix multidentate organic ligands around two metal centers, are analogous to α-helical peptides in size, charge, amphiphilicity, and stereochemistry.[28, 29] It has been demonstrated that these metallohelices can be used as versatile α-helix mimetic structures for stereoselective binding to amyloid proteins and maintaining their nonfibrillar state[30-32]. Additionally, due to their unnatural backbones, these metallohelix exhibit fascinating biological characteristics, such as reduced immunogenicity, resistance to enzymatic hydrolysis, and enhanced bioavailability.[33, 34] Most importantly, the increased diversity in terms of substituents in backbone provides modularity and additional opportunities to introduce chemically functional groups.[28, 29] Encouraged by these perspectives, chiral metallohelix-based chimeras may effectively prevent protein aggregation and direct the nonfibrillar proteins for lysosomal trafficking and subsequent degradation.

As an initial attempt, we explored macrophage galactose-type lectin 1 (MGL1, also known as CD301a) mediated targeted protein degradation using metallohelix-based degraders for extracellular misfolded human islet amyloid polypeptide (hIAPP) associated with type-2 diabetes. MGL1, expressed exclusively by alternatively activated macrophages and dendritic cells (DCs), specifically recognizes glycoproteins expressing terminal galactose (Gal) or N-acetylgalactosamine (GalNAc) residues and triggers phagocytosis and signaling.[35-40] Ligands for MGL1 are also readily available. Molecules that bearing three or more galactose-type sugars showed strong binding affinity to MGL1[41-43]. Therefore, we designed and synthesized metallohelix with triplex architecture to extend MGL binding ligands (GalNAc) into a space that would fit a

trimeric receptor complex. We chose hIAPP, a highly amyloidogenic peptide hormone[44], as a therapeutic target to perform a proof-of-concept experiment. The resulting degraders could be used as a tool to drive the degradation of hIAPP by using a 2-step strategy: first, prevent hIAPP aggregation by stabilizing hIAPP in its nonfibrillar structure; second, induce the spatial proximity between hIAPP and cell-surface MGL, which results in the lysosomal trafficking and degradation of hIAPP peptides (**Scheme** 1). We further confirmed that the enhanced hIAPP elimination was through the endosome/lysosome degradation pathway and dependent on MGL1-mediated endocytosis. Intriguingly, Λ enantiomers showed even higher efficiency in preventing hIAPP aggregation and promoting clearance of hIAPP than Δ enantiomers. Besides, the asialoglycoprotein receptor (ASGPR) contains a carbohydrate-recognition domain (CRD) that is homologous to the CRD of MGL, and thus, also exhibits strong affinity for tri-GalNAc ligand. Not surprisingly, metallohelix-based degraders also faciltated the clearance of hIAPP through ASGPR in liver cells. Taken together, our results demonstrated that chiral-metallohelix could be employed for chiral recognition and degradation of aggregation-prone proteins.

RESULTS AND DISCUSSION

The tri-GalNAc functionalized metallohelix enantiomers (Λ1 and Δ1) were synthesized and characterized as described previously.[34] As shown in **Figure 1**b, circular dichroism (CD) spectra of Λ1 showed exactly mirror image with its enantiomer Δ1, indicating that the chiral structures were successfully synthesized. Furthermore, Λ1 and Δ1 had excellent stability in water, phosphate buffer saline (PBS), and Dulbecco's modified eagle medium (DMEM) (**Figure 1**c and **Figure 1**d) and even undecomposed in PBS buffer over one month (**Figure S**1). Besides, acetylated galactose

(Ac-Gal) and β-galactose (Gal) functionalized metallohelix enantiomers (Λ2 and Δ2, Λ3 and Δ3) were also synthesized and used as controls (**Figure S**2 and **Figure S**3).

Metallohelix inhibited hIAPP aggregation with enantioselectivity. We first explored whether the metallohelices could inhibit hIAPP fibrillation. Transmission electron microscopy (TEM) was used to detect the morphology of hIAPP. Large branched fibrils were observed in the samples of hIAPP alone after incubating at 37 °C for 24 h (**Figure 2**a). Howbeit, in the presence of the metallohelices, hIAPP formed numerous small, relatively amorphous structures, indicating that the metallohelices effectively suppressed the amyloid fibril formation.

The prevention of the hIAPP fibril formation by metallohelices was further substantiated by CD spectroscopy (**Figure 2**b-d). The fresh-prepared monomeric hIAPP alone changed its conformation from random coil to β-sheet structure after 24 h, characterized by a negative peak at 216 nm[45]. In contrast, the intensity of the negative peak at 216 nm decreased substantially in the hIAPP/metallohelices mixture under the identical conditions, indicating that the conversion of hIAPP monomers into β-sheet-rich aggregates was strongly inhibited by metallohelices.

We next measured median inhibitory concentration (IC_{50}) of the six chiral metallohelices on hIAPP aggregation by using thioflavin T (ThT) fluorescence assay[28]. As shown in Figure S4, the metallohelices alone did not influence ThT fluorescence under our experimental conditions. When hIAPP was incubated alone, a sigmoidal curve was observed, which is typical of hIAPP fibrillation[46]. ThT fluorescence intensity increased sharply due to the growth of β-sheet secondary structures. However, in the presence of the metallohelices, ThT fluorescence was hardly changed, implying the metallohelices could prevent hIAPP aggregation (**Figure S**5), and the inhibition in a dose-dependent manner (**Figure S**6). IC_{50} values were estimated 8.32 μM for Λ1, 16.39 μM for Δ1, 18.97 μM for Λ2, 18.4 μM for Δ2, 13.17 μM for Λ3 and 17.38 μM for Δ3. Intriguingly, there

were two features for the metallohelices to prevent hIAPP aggregation. First, the metallohelices with more hydrogen-bond donor groups were more effective. Second, Λ enantiomers showed even stronger inhibition effects than Δ enantiomers[28, 47].

To better understand the different inhibiting capacities of the metallohelices, we performed competition dialysis experiments to reveal the enantiomeric selectivity of metallohelices[29]. The racemic mixture was dialyzed against hIAPP, and the dialysate was monitored by CD spectroscopy (**Figure 3**a-c). The dialysate was enriched in Δ1, Δ2, and Δ3, respectively. These results suggested that hIAPP bound more tightly to Λ enantiomers than Δ enantiomers.

ESI-MS was also employed to compare the binding affinity of the metallohelices to hIAPP. We took Λ3 and Δ3 as examples. hIAPP showed three peaks at 789, 976, and 1301, corresponding to the 5+, 4+ and 3+ ionization states of hIAPP monomer, respectively. However, extra peak was found at 996 (6+ ionization states) in the metallohelices/hIAPP mixture, which corresponded to the 1:1 metallohelices−hIAPP monomer complex (**Figure S**7). More importantly, after treatment of hIAPP with Λ3, the peak of Λ3−hIAPP complex was stronger than that of Δ3−hIAPP complex, further supporting that hIAPP bound more tightly to Λ enantiomers than Δ enantiomers.

To further reinforce these observations, we measured the binding affinities of these metallohelices to hIAPP by using the isothermal titration calorimetry (ITC) and fluorescence titrations. According to the ITC data (**Figure 3**d-i and **Table S**1), the binding was exothermic and gave the best fit to 1:1 binding stoichiometry. Moreover, tri-GalNAc functionalized metallohelices showed stronger binding affinity to hIAPP than other carbohydrate-modified metallohelices. The apparent binding constants (K_a) of Λ1 was $5.54 \times 10^6\ M^{-1}$, which was 3.7-fold stronger than that of Δ1 ($1.50 \times 10^6\ M^{-1}$), showing enantioselectivity. These results were further supported by fluorescence titration experiments (**Figure S**8). All these results inferred that the different

inhibition effects of these metallohelices could be assigned to their different binding affinities to hIAPP.

Moreover, as shown in **Figure S**9, no change was observed by monitoring the absorption at the metal-to-ligand charge transfer (MLCT) band of these metallohelices upon hIAPP binding, implying that the rigid structure of metallohelix was unperturbed by incubation with hIAPP.

Metallohelix promotes macrophage internalization and degradation of hIAPP. Macrophages are major components of the immune defense system and capable of catabolizing aberrant or misfolded proteins from the circulation.[48] The macrophage galactose-type lectin (MGL1), the lectin expressed exclusively by macrophages and dendritic cell (DCs), rapidly clears endogenous glycoproteins terminating in Gal or GalNAc glycans.[39] Therefore, we tested the cellular accumulation of these sugar-appended metallohelices. Alternatively activated RAW264.7 cells (M2 phenotype) were used and cultured with metallohelices (5 μM) for 4 h, and Fe content was detected by using ICP-MS. The Fe content in macrophages cultured with Λ1 or Δ1 was higher than in other groups (**Figure S**10a), which could be attributed to the galactose-mediated endocytosis between tri-GalNAc substituent and MGL1 expressed by macrophages. Notably, the lowest cellular uptake of Λ2/Δ2 was observed, indicating that metallohelices with Ac-Gal substituent couldn't be ingested by MGL1-dependent endocytosis. To further verify that the internalization of Λ1 or Δ1 was mediated through MGL1, excess MGL1 ligands, lactobionic acid or β-galactose, were added to compete for the receptor with metallohelices. After preincubation with competitive ligands, the Fe content in cells became lower because lactobionic acid or β-galactose could saturate MGL1 and further inhibit the galactose-mediated endocytosis (**Figure S**10b). These results suggested that the cellular entry of these sugar-functionalized metallohelices

was mainly MGL1-mediated. Since Λ1 and Δ1 could undergo galactose-mediated endocytosis, and also prevent hIAPP aggregation, we chose Λ1 and Δ1 for further studies.

Before the following experiments, we performed methyl thiazolyl tetrazolium (MTT) assay to evaluate the biological safety of these metallohelices. As shown in **Figure S**11, Λ1 and Δ1 had negligible cytotoxicity towards RAW264.7 cells and MIN6 cells with a concentration of up to 20 μM, suggesting their excellent biocompatibility.

Next, we explored whether these metallohelices could trigger internalization of hIAPP via MGL1-dependent endocytosis. RAW264.7 cells were incubated with either hIAPP or hIAPP/metallohelices (Λ1 or Δ1) mixtures for 4 h, the ingested fluorescently labeled hIAPP (hIAPP-FITC) was analyzed by flow cytometry. As shown in **Figure 4**a and **Figure** 4b, internalization was found dependent on the concentration of the metallohelices, and the maximum internalization was reached at concentration of 5 μM, and this degree of internalization persisted at higher concentrations (10 μM).[14] Intriguingly, chirality differences in uptake efficiency was also observed. Co-incubation with the metallohelices increased cellular hIAPP-FITC by 3.6-fold and 2.4-fold for Λ1 and Δ1, respectively (**Figure 4**c). The better internalizing efficiency of Λ1 was contributed to the higher binding affinity between hIAPP and Λ1.

The effect of metallohelices on macrophage uptake and clearance of hIAPP was also visualized via confocal laser scanning microscopy (CLSM). As macrophages expressed scavenger receptors that can capture hIAPP[48], it was no surprise to see internalization of hIAPP in the absence of metallohelices. In the presence of metallohelices, the co-localization of hIAPP (green) with Lysotracker (red) was prominently increased, indicating that the metallohelices could capture and translocate hIAPP into the endosomes and lysosomes (**Figure 4**d and **Figure 4**e). In conclusion,

co-incubation of hIAPP and the metallohelices inhibited hIAPP aggregation and further facilitated the lysosomal transport of hIAPP.

To rule out the possibility that hIAPP aggregation inhibitor contributes to target internalization, Λ2 with Ac-Gal substituent which could inhibit hIAPP aggregation (**Figure 2**a and **Figure 2**c) but couldn't be ingested by MGL1-dependent endocytosis (**Figure S**10a), was used for verification. As shown in **Figure S**12, compared with that of hIAPP alone-treated cells, no significant improvement in lysosomal hIAPP content was observed for the cells treated with Λ2/hIAPP mixtures as revealed by the green fluorescence of hIAPP. By contrast, for the cells treated with Λ1/hIAPP, large amounts of hIAPP were found co-localization with lysosomes. Consistently, flow cytometry (FCM) analysis disclosed increased internalization of Λ1/hIAPP in comparison to Λ2/hIAPP and hIAPP control (**Figure S**13). These results demonstrated that the inhibitory effect of Λ1 on hIAPP misfolding was not the main reason for the enhanced cellular uptake of hIAPP.

Cleavage sites of amyloid proteins are usually embedded inside the β-sheet structures that limit access by proteases, which would lead to the poor ability of lysosomes to degrade protein aggregates, and further cause lysosomal swelling, destabilization, and dysfunction[22]. To evaluate whether lysosomal-mediated hIAPP degradation occurred, hIAPP-FITC/Λ1 mixtures were incubated with RAW264.7 cells for 4 h, then the cells were washed and cultured in hIAPP-free fresh medium, and cellular hIAPP was detected by FCM. As expected, only small quantities of nonfibrillar hIAPP peptides were found in the hIAPP/Λ1 treated cells after 36 h incubation (**Figure 4**f). Together with the above CLSM images showed co-localization of hIAPP with lysosomes, these data suggested that hIAPP degradation was mediated by lysosomal proteases.

The mechanism of Λ1-mediated hIAPP degradation was further studied, RAW264.7 cells were treated with leupeptin (inhibitor of serine and cysteine proteases) or MG-132 (26 S proteasome

inhibitor). As shown in **Figure 4**g and **Figure S**14, substantial degradation of nonfibrillar hIAPP-FITC was observed in MG-132 treated cells. However, the non-specific inhibition of leupeptin on serine and cysteine proteases resulted in the accumulation of intracellular hIAPP-FITC, suggesting that hIAPP degradation indeed occurred in lysosomes[13, 18]. Similar results were also obtained by ELISA assay (**Figure S**15). Collectively, these results further supported Λ1-mediated hIAPP enrichment in the lysosome and consequent proteolysis.

The ability of lysosomal enzymes to degrade hIAPP in the context of hIAPP/Λ1 mixtures was further confirmed by CLSM (**Figure S**16). As indicated by co-staining of lysosome and hIAPP, cells treated with hIAPP/Λ1 mixtures were sufficient to degrade hIAPP, however, such ability was not found in cells treated with hIAPP fibrils after 24 h incubation (**Figure S**17). Very similar results were obtained by FCM analysis of cellular hIAPP-FITC content (**Figure S**18), which were consistent with previously suggested incomplete and slow degradation process of hIAPP fibrils[48]. These results suggested that nonfibrillar hIAPP/metallohelix mixtures were more efficiently degraded in lysosomes than hIAPP fibrils.

To further explore whether lysosomal damage occurs during the degradation process of hIAPP, we used acridine orange (AO) staining assay to monitored lysosomal integrity.[49, 50] For hIAPP/Λ1-treated cells, bright red fluorescent dots in lysosomes were observed by CLSM (**Figure S**19), which suggested that the lysosomal membranes were integrated. In contrast, the hIAPP alone-treated cells showed weak red fluorescence, indicating that hIAPP fibrils could rupture lysosomal membrane structure and led to lysosomal dysfunction.

Next, we evaluated whether these metallohelices could scavenge amyloid that is endogenously secreted by cells to the extracellular milieu. INS-1-hIAPP cells (upper chamber) were co-cultured with macrophages (bottom chamber) in transwell plates, which allows hIAPP peptides to diffuse

freely between the two chambers. As shown in **Figure S**20, compared with the control groups, re-localization of hIAPP (green) from the plasma membrane to intracellular lysosomes (red) were observed upon Λ1 treatment, suggested that Λ1 could capture and translocate Aβ into lysosomes. Then, substantial degradation of nonfibrillar hIAPP was also observed in Λ1-treated cells as determined by ELISA kits (**Figure S**21). Moreover, hIAPP induced IL-1α and IL-1β production from macrophages was also inhibited by metallohelices. Collectively, Λ1 could scavenge endogenously secreted hIAPP peptides and relieve inflammation.

Mechanism of metallohelices-mediated hIAPP internalization and degradation. To elucidate the internalization mechanism of hIAPP, we treated the RAW264.7 cells with inhibitors of different endocytic pathways[51], including chlorpromazine (CHL, an inhibitor of clathrin-mediated endocytosis) and amiloride (AMI, an inhibitor of macropinocytosis). As indicated by flow cytometry analysis (**Figure S**22, for hIAPP alone-treated cells, inhibitors AMI and CHL resulted in obvious reduction of cellular uptake of hIAPP, indicating hIAPP uptake was mediated by macropinocytosis and clathrin-mediated endocytosis. In contrast, as for hIAPP/Λ1-treated cells, CHL significantly reduced cellular uptake of hIAPP, whereas AMI slightly attenuated the hIAPP internalization. These results indicated that the main cellular uptake of hIAPP/Λ1 could be through clathrin-mediated endocytosis.

Next we testified whether MGL1 receptor was involved in metallohelix-mediated hIAPP degradation. Alternatively activated microphages (M2 phenotype) were pretreated with an inhibiting antibody or an isotype control antibody.[39] As shown in **Figure S**23, hIAPP/Λ1 treatment increased hIAPP internalization by 3.6-fold. Pretreatment with MGL1 inhibitory antibody dramatically impeded the internalization of hIAPP into macrophages, whereas the hIAPP

internalization was unaffected in the IgG-pretreated groups. We then compared the uptake of hIAPP into classically activated microphages (M1 phenotype) with low MGL1 expression levels[40] and found that the amount of hIAPP-FITC was obviously reduced with the decrease of MGL1 level. These results demonstrated that MGL1 receptor played important roles in the metallohelix-mediated hIAPP internalization.[39] Considering that endocytosis mediated by MGL1 is dependent on clathrin[52, 53], these results were consistent with the endocytosis inhibition assay.

To ensure that degradation of hIAPP occurred by MGL1-mediated endocytosis, we tested whether perturbing the interaction with MGL1 would influence hIAPP internalization. Macrophages were pre-treated with siRNA to target MGL1. As shown in **Figure 5**a and **Figure 5**b, Λ1-induced hIAPP internalization was abolished following MGL1 knockdown, while hIAPP uptake proceeded in cells transfected with control siRNA. These results further confirmed that MGL1 played important roles in Λ1-induced hIAPP elimination.

The induced MGL1-hIAPP interaction was also visualized by CLSM. As shown in **Figure 5**c, most hIAPP peptides were observed colocalized with MGL1 receptors in the hIAPP/Λ1-treated cells. In contrast, there was much less colocalization of hIAPP with MGL1 in the hIAPP alone-treated cells. These results further confirmed that the MGL1 receptor was essential for Λ1-mediated hIAPP internalization and clearance.

MGL1 receptor involved in the clearance of IAPP/Λ1 mixtures was also supported by the competitive binding studies using MGL1 binding agent, β-galactose.[38] The fluorescence intensity of hIAPP was decreased with the addition of β-galactose (**Figure S**24), suggesting that hIAPP uptake promoted by Λ1 was attenuated by co-incubation with excess competitive ligands. To substantiate this finding, the internalization of hIAPP was further detected by FCM, and similar results were obtained (**Figure S**25). Furthermore, no detectable improvement in cellular hIAPP

content was observed for macrophages treated with control metallohelices that does not contain GalNAc moieties (**Figure S**26 and **Figure S**27). Collectively, these data suggested the involvement of MGL1 in the transportation of hIAPP and implied that the tri-GalNAc modified metallohelix effectively delivered the targeted protein into macrophages.

Molecular docking simulation on the hIAPP-Λ1-MGL1 ternary complex. To better dissect and understand the interactions between hIAPP-Λ1 and MGL1, we performed molecular docking simulations on the hIAPP-Λ1-MGL1 ternary complex.[54] The hIAPP-MGL1 complexes were first generated using global docking predictions from ZDOCK, and further performing local side-chain and rigid-body refinement using Rosetta.[55, 56] The top 50 preferential poses were used to dock our degrader (Λ1). The resultant low-energy conformation of the hIAPP-Λ1-MGL1 ternary complex was shown in **Figure 6**a. The GalNAc ring of Λ1 had contacts with both LYS1 and ASN3, and another GalNAc ring interacted with THR36 (**Figure 6**b). Moreover, the aryl ring of Λ1 could also produce hydrophobic interactions and π-π-interactions with hydrophobic residues located in the exterior part of hIAPP (**Figure 6**c). These results suggested that such metallohelix provided a multivalent surface for interactions with hIAPP, resulting in its inhibition of hIAPP aggregation. Furthermore, Λ1 binding to MGL1 was involved the interactions of the hydroxyls at C-3 and C-4 of the GalNAc ring with residues of MGL1 (GLN239, ASP241, GLU252, ASN164) and calcium ion, consistent with previous analogue structure and predictions (**Figure 6**d).[57, 58] Through binding to cell-surface lysosome shuttling receptor and the target protein, the resulting hIAPP-Λ1-MGL1 complex was engulfed by the cell membrane, and finally the target protein was degraded in lysosomes. These results provided a possible mechanistic insight into Λ1 how to inhibit hIAPP aggregation and promote hIAPP clearance.

Metallohelix also facilitates the uptake of hIAPP through ASGPR in liver cells.

Asialoglycoprotein receptor (ASGPR) is another well-defined lysosomal shuttling receptor, which is primarily and highly expressed in hepatocytes.[14-16] GalNAc, especially trimeric GalNAc can also bind to ASGPR very potently. Therefore, we explored whether these metallohelices could trigger internalization of hIAPP through ASGPR in HepG2 cells. As shown in **Figure S**28, FCM analysis disclosed increased internalization of hIAPP/Λ1 compared to hIAPP control. CLSM images showed the distribution of hIAPP in the cytoplasm and colocalization with lysosomes (**Figure S**29). Moreover, substantial degradation of nonfibrillar hIAPP was also observed in Λ1-treated HepG2 cells (**Figure S**30). These results implied the metallohelix-mediated uptake and traffic of the hIAPP to the lysosome through ASGPR-dependent manner. Since liver is the major place for protein catabolism, delivering amyloid proteins to the liver for degradation can be potentially advantageous.[14-16]

DISSCUSSION

Until now, many therapeutic inhibitors have been prepared to modulate the aggregation of amyloid proteins, including peptides, small molecules, metal complexes, and even nanoparticles.[28-32] Given the reversible binding of these inhibitors, enough drug concentrations and sustained systemic exposure of the drug are often required to ensure sufficient inhibition. Unfortunately, continuous drug exposure may produce a wide range of on-target toxicity.[24, 25] The emergence of degraders that are capable of depleting POIs through degradation pathways have the potential to overcome drawbacks associated with conventional inhibitors.[1, 2] In the present work, we described our initial proof-of-concept studies using metallohelix-based degraders to deliver the

extracellular hAIPP peptides into the lysosomes for degradation. The deleterious effects associated with the protein aggregates can be effectively blocked through protein degradation strategies. Collectively, targeted amyloid degradation by hybrid metallohelix may provide an alternative modality, fundamentally distinct from current inhibitors, to completely deplete the extracellular protein aggregates.[24, 25]

Exploring new lysosome shuttling receptors will greatly promote development of targeted lysosomal degradation strategy.[12] MGL, expressed primarily by macrophages and DCs, responsible for clearing glycoproteins expressing terminal Gal or GalNAc residues via endo-lysosomal pathway.[35-40] This expression pattern makes MGL a promising lysosomal shuttling receptor for macrophages-mediated protein degradation. In this work, we observed that tri-GalNAc functionalized metallohelices could induce the spatial proximity between hIAPP and cell-surface MGL, which results in the lysosomal trafficking and degradation of hIAPP peptides in macrophages. Our results demonstrated the feasibility of MGL-mediated protein degradation strategy.

C-type lectin receptor (CLEC) is involved in diverse physiological processes, such as glycoprotein turnover, ligand-specific endocytosis and recognition of environmental danger signals.[52, 53] Carbohydrate-recognition domain (CRD) is a predominant property of C-type lectins. Among the CLEC superfamily, two are of particular interest. ASGPR (CLEC4H1), a type II transmembrane CLEC receptor, is expressed nearly exclusively in hepatocytes. MGL (CLEC10A) is another membrane-anchored CLEC receptor that is expressed predominantly by macrophages and DCs. Both lectins contain homologous CRDs that exclusively binds terminal GalNAc residues.[38] In light of this, it is not unexpected that tri-GalNAc functionalized metallohelices also faciltated the clearance of hIAPP through ASGPR in liver cells. Since liver is the major place for

protein catabolism, delivering amyloid proteins to the liver for degradation can be potentially advantageous.[14-16]

STUDY LIMITATIONS

Several limitations existed in the present work. First, metallohelices bind α/β-discordant segments of protein generally, not hIAPP specifically. Our current work explored the effects of metallohelices on the clearance of extracellular protein aggregates but overlooked the possible impacts on normal proteins. However, structural modifications (such as sugar functionalization and incorporate chirality into degraders) greatly increased the binding affinity of metallohelices to hIAPP peptides, which may weaken the off-target effects. This will guide us to do better design and synthesize different types of metallohelices in the future for improving their binding affinity toward specific targets and enantioselectivity. Second, innate receptors such as C-type lectin receptors (CLEC), have been widely investigated in the immune system as they recognize pathogens and play important roles in both innate and adaptive immune responses. Nevertheless, the present work did not consider the potential effect of degraders-induced CLEC activation on immune systems. Finally, the observed hIAPP degradation is heavy reliance on cell-based models that do not closely represent clinical circumstance. Besides, the duration of treatment in cell-based models remains too short to assess the long-term safety as well as the metabolic properties of degraders. Re-optimization of delivery strategy and dosing schedule are needed before *in vivo* animal model studies. Moreover, key factors of metallohelices need to be systematically investigated *in vivo*, such as applicability, selectivity, and potential side effects.

CONCLUSIONS

In the present work, metallohelix-based degraders have been developed to direct extracellular hAIPP peptides toward lysosomal degradation via LTRs. Degraders were composed of LTR binding ligands (tri-GalNAc) and chiral metallohelix. These triplex metallohelices were biocompatible, water-soluble, and stable in water and biological media. Owing to the critical role of α-helical intermediates in amyloid fibril formation, the chiral α-helical mimetic could bind to hIAPP and inhibit aggregation. Most importantly, the addition of the carbohydrate units leads to a significant expansion of their functions. The resulting tri-GalNAc functionalized metallohelix could direct the bound hIAPP for lysosomal trafficking and subsequent degradation. Further studies revealed that metallohelix-based degraders induced the spatial proximity between hIAPP and cell-surface LTR, leading to proteasomal degradation of hIAPP via the endo-lysosomal pathway. Intriguingly, Λ enantiomers showed even higher efficiency in preventing hIAPP aggregation and promoting the elimination of hIAPP than Δ enantiomers. Taker together, our work demonstrated that metallohelix could be employed for targeted degradation of extracellular protein aggregates and possess enantioselectivity.

EXPERIMENTAL DETAILS

Synthesis of metallohelices: Metallohelices were synthesized and characterized according to our previous report.

Protein sample preparation: hIAPP was dissolved in HFIP and stored at -20 °C. Before use, the solvent HFIP was evaporated and hIAPP was redissolved in 20 mM Tris buffer (pH 7.4). For the hIAPP aggregation, the solution was incubated at 37 °C for 24 hours.

hIAPP uptake and degradation: 1 day-aged solutions of hIAPP or hIAPP/metallohelices in PBS buffer (pH 7.4) were diluted with cell culture medium and added to the cells at a final peptide concentration of 5 μM. After incubation for 4 h, LysoTracker Red (Beyotime) was used to stain lysosomes. After staining for 15 min, PBS was used to wash cells and 4% formaldehyde was used to fix cells. Finally, the cell nuclei were stained by DAPI and hIAPP peptides were stained with antibodies (Santa Cruz Biotechnology, sc-377530). After 15 min, cells were washed with PBS and observed by laser scanning confocal microscopy. For flow cytometry (FCM) analysis, hIAPP-FITC were used instead of hIAPP peptides**.**

After hIAPP/Λ1 mixture treatment, cells were washed with PBS and cultured in hIAPP-free fresh medium to allow further degradation. At varying times thereafter, the cells were thoroughly washed and trypsinized to digest surface-bound hIAPP, followed by lysis, and intracellular hIAPP was quantified by FCM or ELISA kits (Energy Chemical, EL0518).

Protease inhibition experiments: Cells were incubated with hIAPP/Λ1 mixture for 4 h followed by three washes with PBS. Cells were maintained subsequently in fresh media with leupeptin (Solarbio, L8110) or MG-132 (Shandong Sparkjade Biotechnology Co., Ltd., SJ-BP0049A) for 6 h, 12 h, 24 h, and 36 h. The samples lacking protease inhibitors were treated with 1% DMSO as a vehicle control.

Endocytosis inhibition assay: Activated macrophages were exposed to chlorpromazine (MCE, HY-12708) or amiloride (MCE, HY-B0285) and incubated for 30 min at 37°C. 1 day-aged solutions of hIAPP-FITC or hIAPP-FITC/metallohelices in PBS buffer (pH 7.4) were diluted with cell culture medium and added to the cells at a final peptide concentration of 5 μM. The internalized hIAPP was quantified using FCM.

Antibody inhibition experiments: Activated macrophages were pretreated with an inhibiting antibody (Santa Cruz Biotechnology, sc-56109) or an isotype control antibody (rat IgG2a) for 6 h, then incubated with hIAPP-FITC or hIAPP-FITC/Λ1 mixtures for 4 h. The level of endocytosed hIAPP were analyzed by FCM.

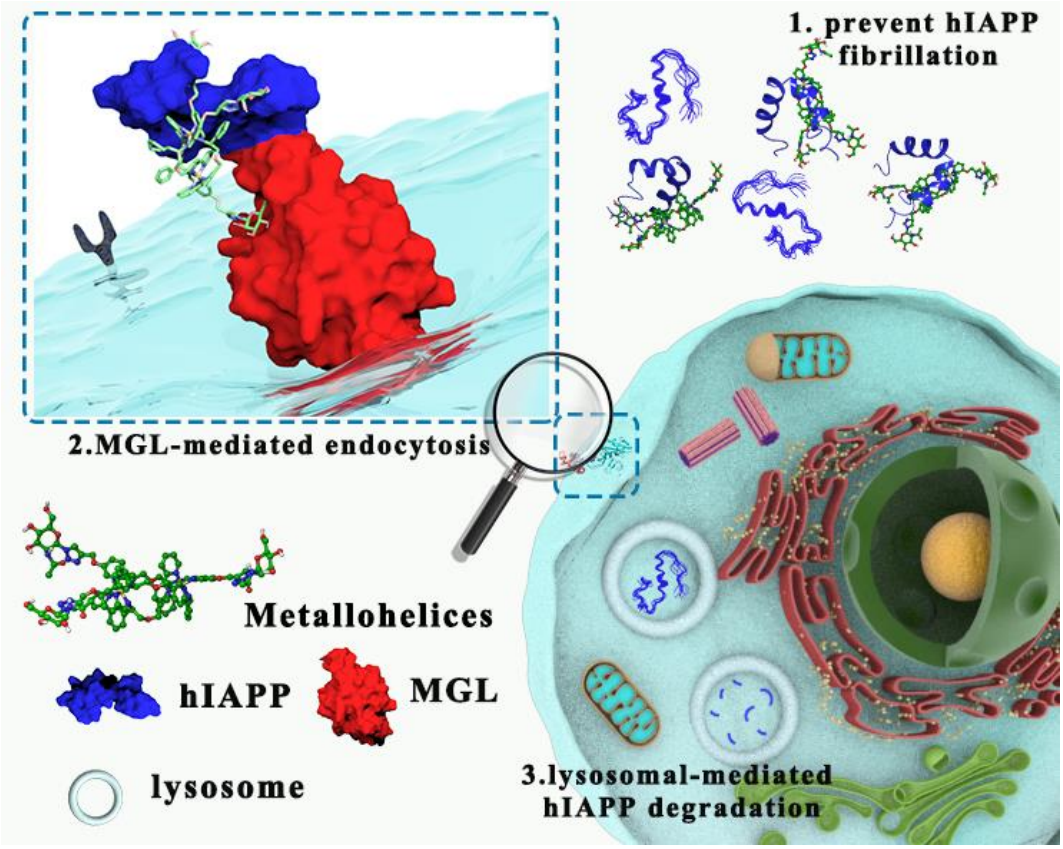

Scheme 1. Mechanism of action of metallohelix-based degraders. On simultaneously binding to both MGL1 and hIAPP, the resulting ternary complex is engulfed by the cell membrane, which forms a transport vesicle. Finally, hIAPP is transported to lysosomes and degraded.

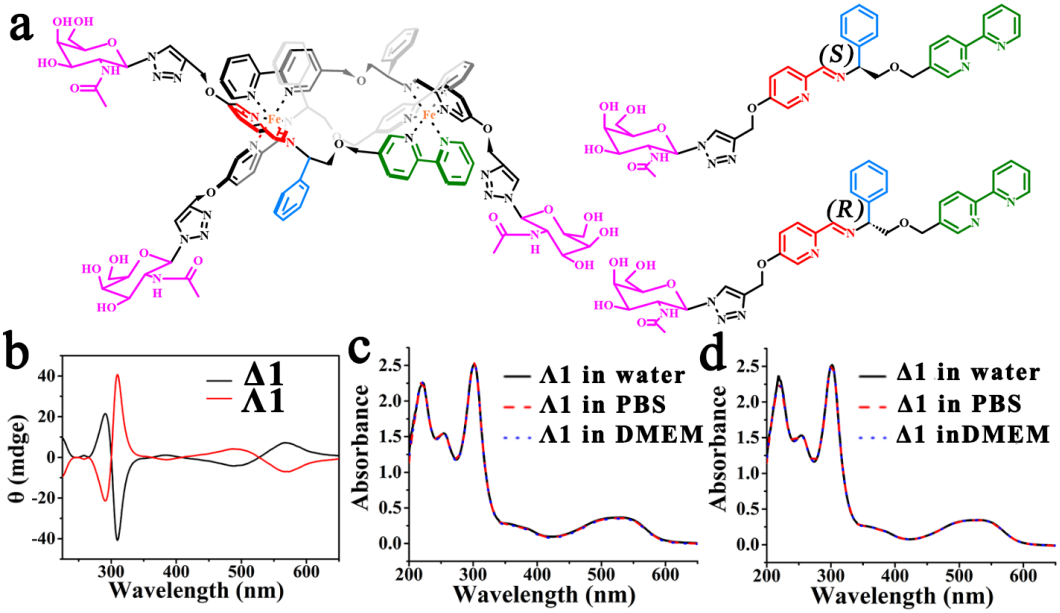

Figure 1. (a) Characterization of tri-GalNAc functionalized metallohelices. **(b)** CD spectra of Λ1 (red) and Δ1 (black) (40 μM in H_2O). UV-vis absorption spectra of Λ1 **(c)** and Δ1 **(d)** in water, PBS, and DMEM.

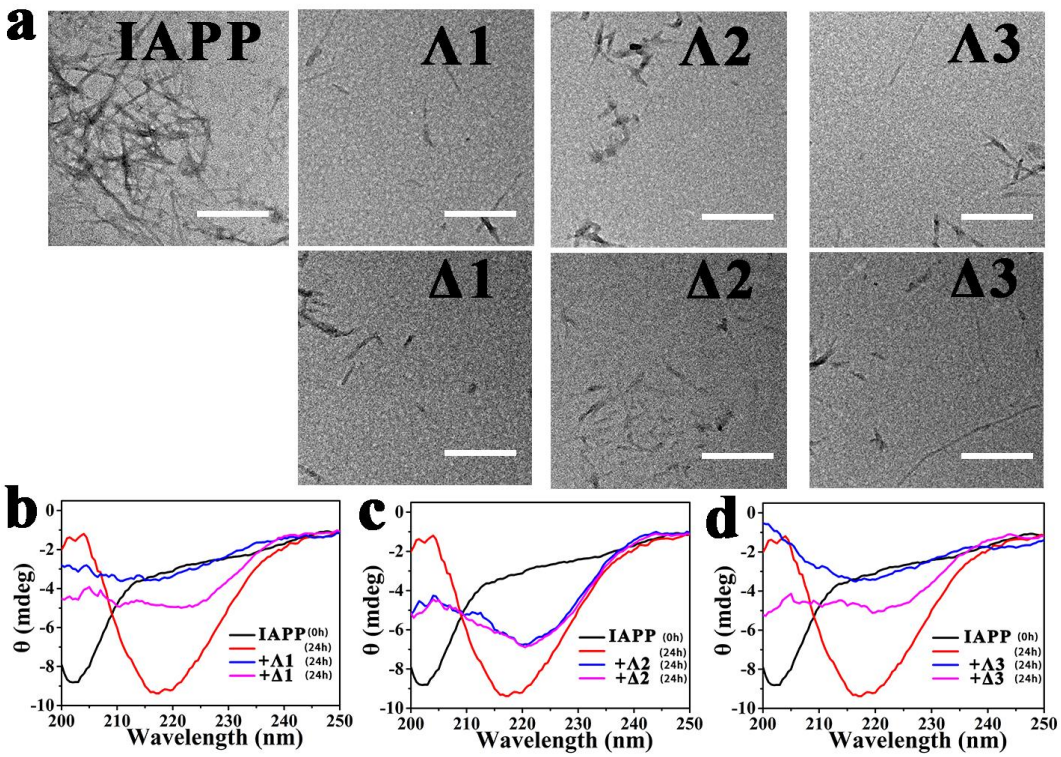

Figure 2. hIAPP aggregation in the absence or presence of metallohelices. The hIAPP (20 μM) or hIAPP (20 μM)/metallohelices (20 μM) mixtures were measured in 10 mM HEPES (pH 7.3) after incubation at 37 °C for 24 h. **(a)** TEM images of hIAPP with or without incubation of metallohelices. Scale bars are 250 nm. **(b-d)** The aggregation behavior of hIAPP was monitored by CD spectra in the absence or presence of metallohelices.

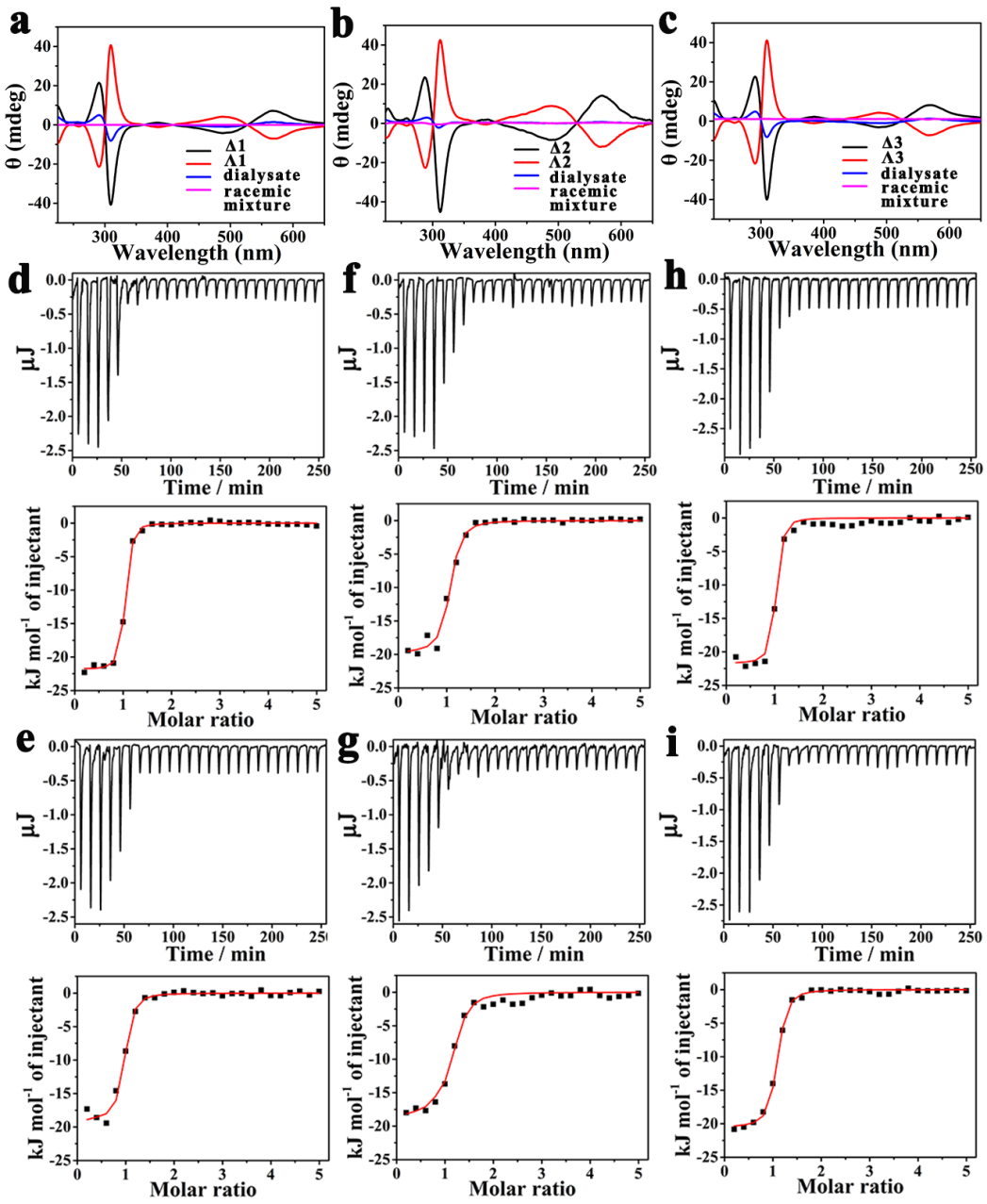

Figure 3. Λ enantiomers showed higher binding affinity to hIAPP than Δ enantiomers. **(a-c)** Competition dialysis experiment. CD spectroscopy was used to monitor the dialysate. **(d-i)** Representative ITC data for the interactions between chiral metallohelices and hIAPP, Λ1 **(d)**, Δ1 **(e)**, Λ2 **(f)**, Δ2 **(g)**, Λ3 **(h)**, Δ3 **(i)**.

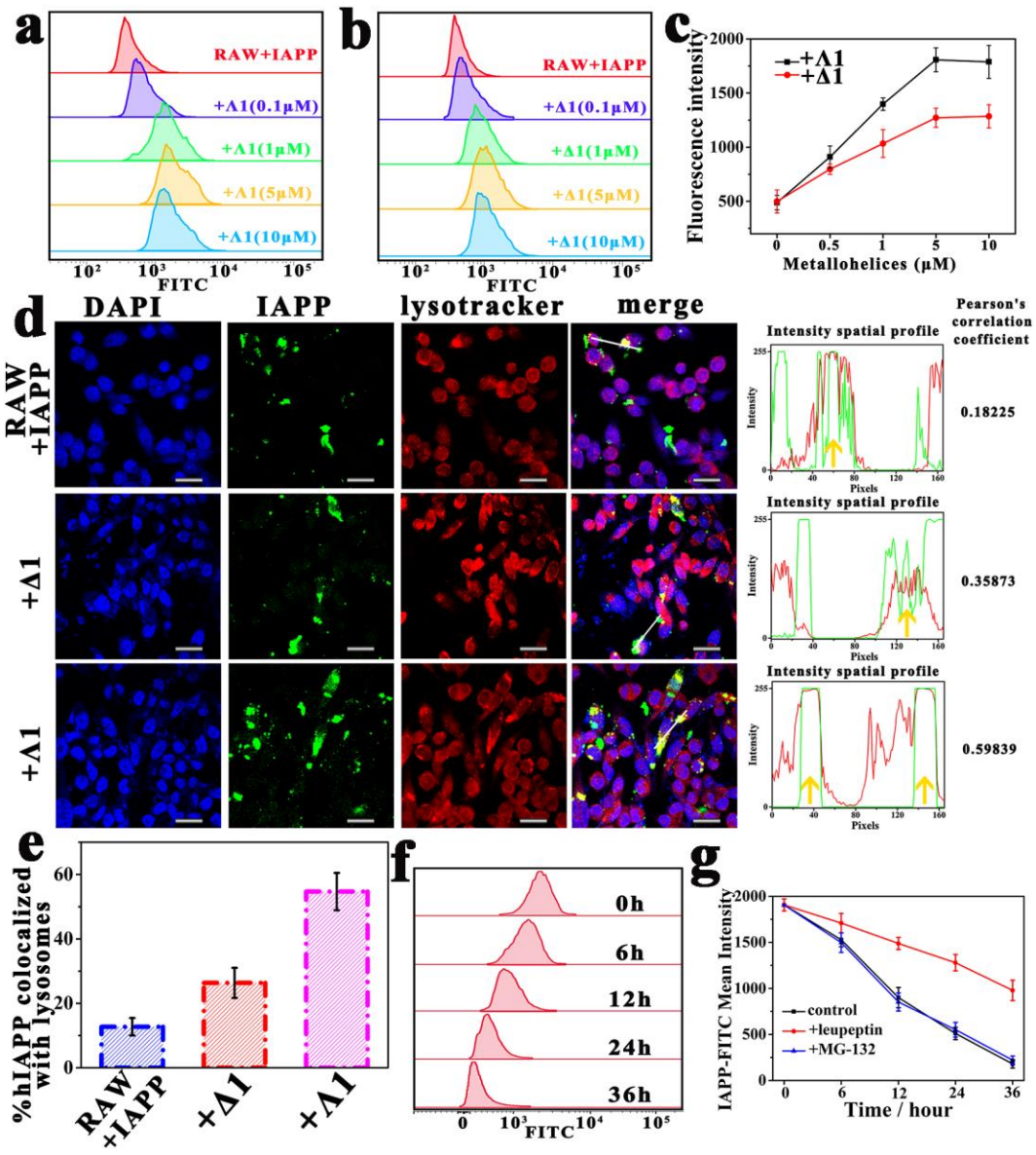

Figure 4. Metallohelix-based degraders promoted clearance of hIAPP in RAW264.7 cell lines. Internalization of hIAPP-FITC in macrophages determined by FCM following 4 h treatment with Λ1 **(a)** or Δ1 **(b)** at different concentrations. **(c)** Internalization of hIAPP in RAW264.7 cells evaluated by flow cytometry under different conditions. Mean fluorescence intensity (MFI) was measured by flow cytometry. **(d)** Representative images of hIAPP internalization in macrophages by confocal microscopy after hIAPP (5 μM)/metallohelices (5 μM) treatments for 4 h. hIAPP peptides were stained with antibodies (green), lysosome was stained with lysotracker red (red),

and DNA was stained with DAPI (blue). Yellow areas indicated co-localization of hIAPP and lysosomes. Scale bars are 20 μm. Images are representative of two independent experiments. **(e)** The percentage of hIAPP peptides that are colocalized with lysosomes in each sample (n = 3, independent experiments) was analyzed by Nikon colocalization software. **(f)** Degradation of hIAPP-FITC peptides in the hIAPP/Λ1 treated cells. After incubated with hIAPP-FITC/Λ1 mixtures for 4 h, the degradation of hIAPP for 6 to 36 h were measured by FCM. **(g)** The degradation of hIAPP-FITC for 6 to 36 h in the presence of leupeptin (red) or MG-132 (blue) were detected by FCM.

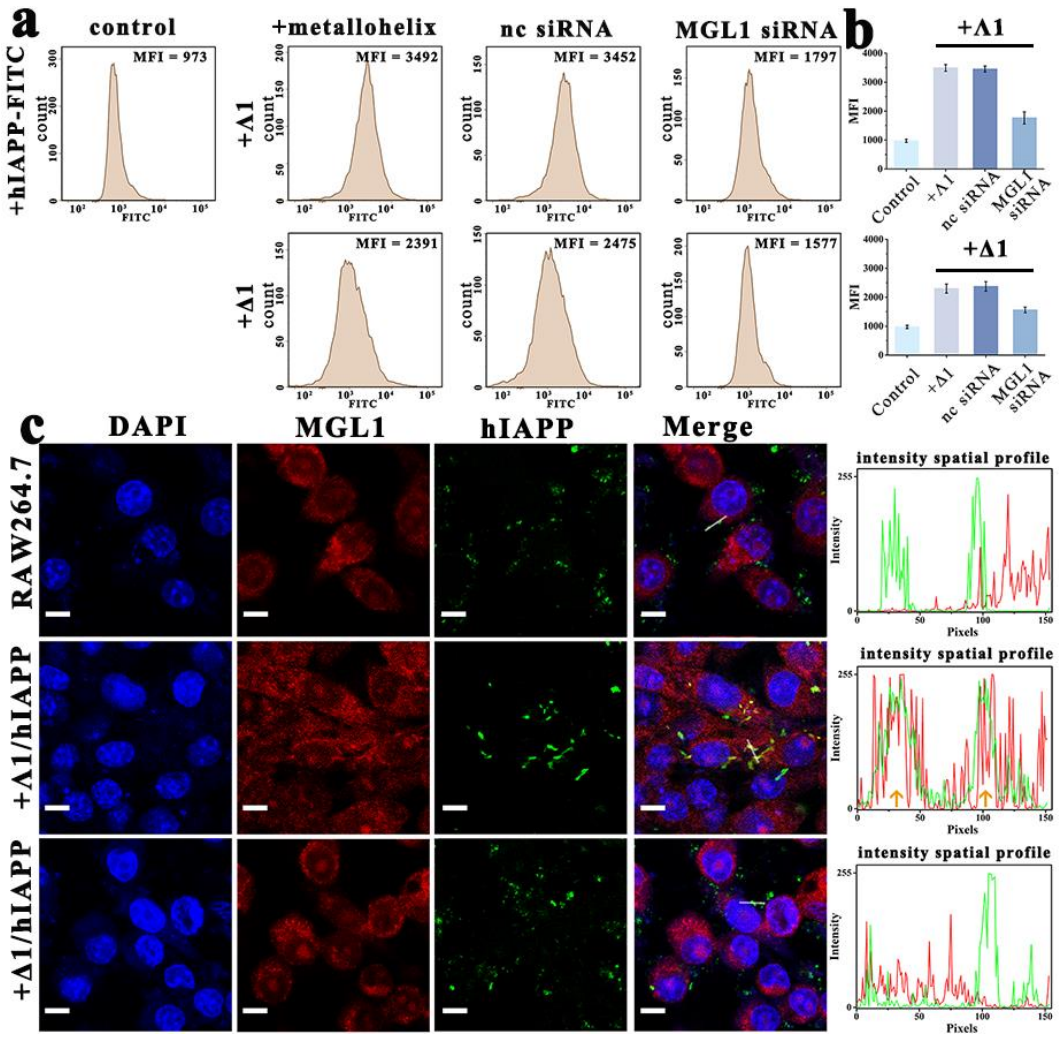

Figure 5. Mechanism of metallohelices-mediated internalization. Λ1/hIAPP mixtures bound to macrophages MGL1 receptors and were internalized by receptor-mediated endocytosis. **(a)** Cellular hIAPP levels were determined by FCM in macrophages following knockdown of MGL1 by siRNA. Negative control siRNA was used as a control. **(b)** Mean fluorescence intensity (MFI) was determined by live cell FCM. Values are the average of three independent experiments. **(c)** Confocal images of RAW264.7 cells incubated with hIAPP were stained with antibodies against hIAPP (green) and MGL1 (red); DNA was stained with DAPI (blue). Arrows indicate co-localization of hIAPP and MGL1.

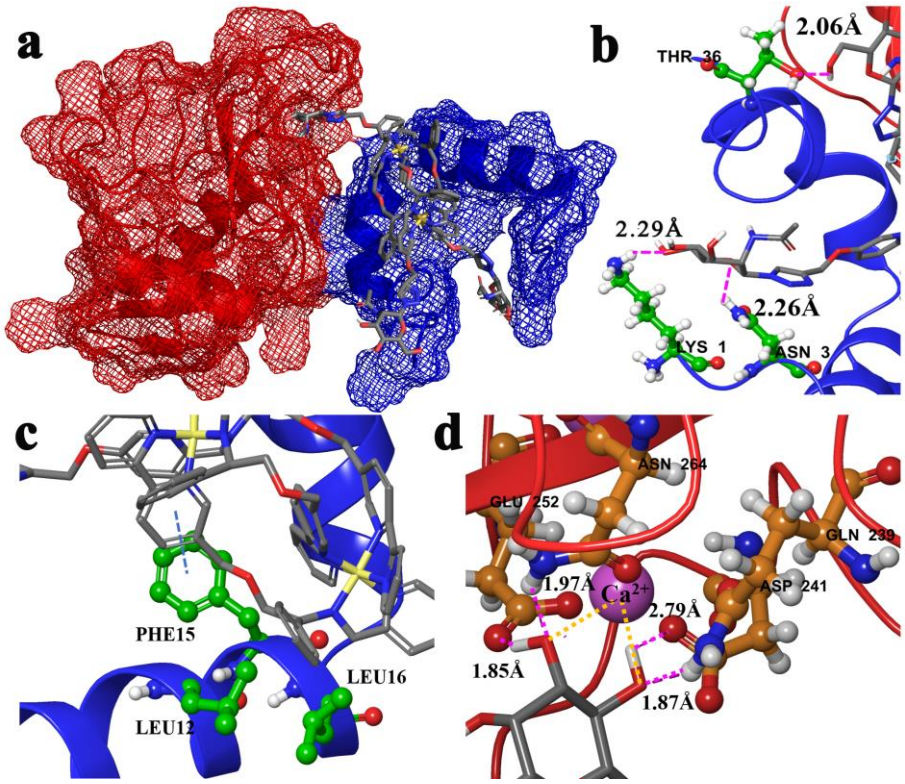

Figure 6. **(a)** Docking pose of the hIAPP-Λ1-MGL1 ternary complex. The cartoon and surface of hIAPP are displayed in blue, whereas the cartoon and surface of MGL1 are displayed in red. Λ1 is colored gray. **(b-c)** Predicted binding mode for Λ1 (gray) with hIAPP. Hydrogen bonds and π-π-interactions are shown in dashes. **(d)** Predicted binding mode for Λ1 (gray) with MGL1 at the hIAPP-Λ1-MGL1 ternary complex. Hydrogen bonds and bonds to metal ion (purple sphere) are shown in dashes.

ASSOCIATED CONTENT

Supporting Information.

The Supporting Information is available free of charge *via* the Internet at http://pubs.acs.org. Materials, measurements, experimental details of metallohelix-mediated hIAPP internalization and degradation, Figure S1-S30, Table S1-S2.

AUTHOR INFORMATION

Corresponding Author

*E-mail: xqu@ciac.ac.cn

ACKNOWLEDGMENT

Financial support was provided by the National Key R&D Program of China (2019YFA0709202 and 2021YFF1200700), and National Natural Science Foundation of China (91856205, 21820102009 and 22237006).

REFERENCES

(1) Lai, A. C.; Crews, C. M., Induced protein degradation: an emerging drug discovery paradigm. *Nat. Rev. Drug Discov.* **2017,** *16*, 101-114.

(2) Verma, R.; Mohl, D.; Deshaies, R. J., Harnessing the Power of Proteolysis for Targeted Protein Inactivation. *Mol. Cell* **2020,** *77*, 446-460.

(3) Clift, D.; McEwan, W. A.; Labzin, L. I.; Konieczny, V.; Mogessie, B.; James, L. C.; Schuh, M., A Method for the Acute and Rapid Degradation of Endogenous Proteins. *Cell* **2017,** *171*, 1692-1706 e18.

(4) Winter, G. E.; Buckley, D. L.; Paulk, J.; Roberts, J. M.; Souza, A.; Dhe-Paganon, S.; Bradner, J. E., DRUG DEVELOPMENT. Phthalimide conjugation as a strategy for in vivo target protein degradation. *Science* **2015,** *348*, 1376-1381.

(5) Burslem, G. M.; Crews, C. M., Proteolysis-Targeting Chimeras as Therapeutics and Tools for Biological Discovery. *Cell* **2020,** *181*, 102-114.

(6) Nabet, B.; Roberts, J. M.; Buckley, D. L.; Paulk, J.; Dastjerdi, S.; Yang, A.; Leggett, A. L.; Erb, M. A.; Lawlor, M. A.; Souza, A.; Scott, T. G.; Vittori, S.; Perry, J. A.; Qi, J.; Winter, G. E.; Wong, K. K.; Gray, N. S.; Bradner, J. E., The dTAG system for immediate and target-specific protein degradation. *Nat. Chem. Biol.* **2018,** *14*, 431-441.

(7) Lu, J.; Qian, Y.; Altieri, M.; Dong, H.; Wang, J.; Raina, K.; Hines, J.; Winkler, J. D.; Crew, A. P.; Coleman, K.; Crews, C. M., Hijacking the E3 Ubiquitin Ligase Cereblon to Efficiently Target BRD4. *Chem. Biol.* **2015,** *22*, 755-763.

(8) Takahashi, D.; Moriyama, J.; Nakamura, T.; Miki, E.; Takahashi, E.; Sato, A.; Akaike, T.; Itto-Nakama, K.; Arimoto, H., AUTACs: Cargo-Specific Degraders Using Selective Autophagy. *Mol. Cell* **2019,** *76*, 797-810 e10.

(9) Li, Z.; Wang, C.; Wang, Z.; Zhu, C.; Li, J.; Sha, T.; Ma, L.; Gao, C.; Yang, Y.; Sun, Y.; Wang, J.; Sun, X.; Lu, C.; Difiglia, M.; Mei, Y.; Ding, C.; Luo, S.; Dang, Y.; Ding, Y.; Fei, Y.; Lu, B., Allele-selective lowering of mutant HTT protein by HTT-LC3 linker compounds. *Nature* **2019,** *575*, 203-209.

(10) Fan, X.; Jin, W. Y.; Lu, J.; Wang, J.; Wang, Y. T., Rapid and reversible knockdown of endogenous proteins by peptide-directed lysosomal degradation. *Nat. Neurosci.* **2014,** *17*, 471-480.

(11) Bauer, P. O.; Goswami, A.; Wong, H. K.; Okuno, M.; Kurosawa, M.; Yamada, M.; Miyazaki, H.; Matsumoto, G.; Kino, Y.; Nagai, Y.; Nukina, N., Harnessing chaperone-mediated autophagy for the selective degradation of mutant huntingtin protein. *Nat. Biotechnol.* **2010,** *28*, 256-263.

(12) Alabi, S.; Crews, C., Major Advances in Targeted Protein Degradation: PROTACs, LYTACs, and MADTACs. *J. Biol. Chem.* **2021,** *296*, 100647.

(13) Banik, S. M.; Pedram, K.; Wisnovsky, S.; Ahn, G.; Riley, N. M.; Bertozzi, C. R., Lysosome-targeting chimaeras for degradation of extracellular proteins. *Nature* **2020,** *584*, 291-297.

(14) Ahn, G.; Banik, S. M.; Miller, C. L.; Riley, N. M.; Cochran, J. R.; Bertozzi, C. R., LYTACs that engage the asialoglycoprotein receptor for targeted protein degradation. *Nat. Chem. Biol.* **2021,** *17*, 937-946.

(15) Zhou, Y.; Teng, P.; Montgomery, N. T.; Li, X.; Tang, W., Development of Triantennary N-Acetylgalactosamine Conjugates as Degraders for Extracellular Proteins. *ACS Cent. Sci.* **2021,** *7*, 499-506.

(16) Caianiello, D. F.; Zhang, M.; Ray, J. D.; Howell, R. A.; Swartzel, J. C.; Branham, E. M. J.; Chirkin, E.; Sabbasani, V. R.; Gong, A. Z.; McDonald, D. M.; Muthusamy, V.; Spiegel, D. A., Bifunctional small molecules that mediate the degradation of extracellular proteins. *Nat. Chem. Biol.* **2021,** *17*, 947-953.

(17) Cotton, A. D.; Nguyen, D. P.; Gramespacher, J. A.; Seiple, I. B.; Wells, J. A., Development of Antibody-Based PROTACs for the Degradation of the Cell-Surface Immune Checkpoint Protein PD-L1. *J. Am. Chem. Soc.* **2021,** *143*, 593-598.

(18) Miao, Y.; Gao, Q.; Mao, M.; Zhang, C.; Yang, L.; Yang, Y.; Han, D., Bispecific Aptamer Chimeras Enable Targeted Protein Degradation on Cell Membranes. *Angew. Chem. Int. Ed.* **2021,** *60*, 11267-11271.

(19) Zhang, H.; Han, Y.; Yang, Y.; Lin, F.; Li, K.; Kong, L.; Liu, H.; Dang, Y.; Lin, J.; Chen, P. R., Covalently Engineered Nanobody Chimeras for Targeted Membrane Protein Degradation. *J. Am. Chem. Soc.* **2021,** *143*, 16377-16382.

(20) Butterfield, D. A.; Halliwell, B., Oxidative stress, dysfunctional glucose metabolism and Alzheimer disease. *Nat. Rev. Neurosci.* **2019,** *20*, 148-160.

(21) Pluvinage, J. V.; Haney, M. S.; Smith, B. A. H.; Sun, J.; Iram, T.; Bonanno, L.; Li, L.; Lee, D. P.; Morgens, D. W.; Yang, A. C.; Shuken, S. R.; Gate, D.; Scott, M.; Khatri, P.; Luo, J.; Bertozzi, C. R.; Bassik, M. C.; Wyss-Coray, T., CD22 blockade restores homeostatic microglial phagocytosis in ageing brains. *Nature* **2019,** *568*, 187-192.

(22) Halle, A.; Hornung, V.; Petzold, G. C.; Stewart, C. R.; Monks, B. G.; Reinheckel, T.; Fitzgerald, K. A.; Latz, E.; Moore, K. J.; Golenbock, D. T., The NALP3 inflammasome is involved in the innate immune response to amyloid-beta. *Nat. Immunol.* **2008,** *9*, 857-865.

(23) Heckmann, B. L.; Teubner, B. J. W.; Tummers, B.; Boada-Romero, E.; Harris, L.; Yang, M.; Guy, C. S.; Zakharenko, S. S.; Green, D. R., LC3-Associated Endocytosis Facilitates beta-Amyloid Clearance and Mitigates Neurodegeneration in Murine Alzheimer's Disease. *Cell* **2019,** *178*, 536-551 e14.

(24) Tomoshige, S.; Nomura, S.; Ohgane, K.; Hashimoto, Y.; Ishikawa, M., Discovery of Small Molecules that Induce the Degradation of Huntingtin. *Angew. Chem. Int. Ed.* **2017,** *56*, 11530-11533.

(25) Tomoshige, S.; Ishikawa, M., PROTACs and Other Chemical Protein Degradation Technologies for the Treatment of Neurodegenerative Disorders. *Angew. Chem. Int. Ed.* **2021,** *60*, 3346-3354.

(26) Hwang, W. Y.; Foote, J., Immunogenicity of engineered antibodies. *Methods* **2005,** *36*, 3-10.

(27) Ma, M.; Wang, Y.; Gao, N.; Liu, X.; Sun, Y.; Ren, J.; Qu, X., A Near-Infrared-Controllable Artificial Metalloprotease Used for Degrading Amyloid-beta Monomers and Aggregates. *Chemistry* **2019,** *25*, 11852-11858.

(28) Guan, Y.; Du, Z.; Gao, N.; Cao, Y.; Wang, X.; Scott, P.; Song, H.; Ren, J.; Qu, X., Stereochemistry and amyloid inhibition: Asymmetric triplex metallohelices enantioselectively bind to Aβ peptide. *Sci. Adv.* **2018,** *4*, eaao6718.

(29) Li, M.; Howson, S. E.; Dong, K.; Gao, N.; Ren, J.; Scott, P.; Qu, X., Chiral metallohelical complexes enantioselectively target amyloid beta for treating Alzheimer's disease. *J. Am. Chem. Soc.* **2014,** *136*, 11655-11663.

(30) Saraogi, I.; Hebda, J. A.; Becerril, J.; Estroff, L. A.; Miranker, A. D.; Hamilton, A. D., Synthetic alpha-helix mimetics as agonists and antagonists of islet amyloid polypeptide aggregation. *Angew. Chem., Int. Ed.* **2010,** *49*, 736-739.

(31) Fremaux, J.; Mauran, L.; Pulka-Ziach, K.; Kauffmann, B.; Odaert, B.; Guichard, G., alpha-Peptide-Oligourea Chimeras: Stabilization of Short alpha-Helices by Non-Peptide Helical Foldamers. *Angew. Chem., Int. Ed.* **2015,** *54*, 9816-9820.

(32) De Carufel, C. A.; Quittot, N.; Nguyen, P. T.; Bourgault, S., Delineating the Role of Helical Intermediates in Natively Unfolded Polypeptide Amyloid Assembly and Cytotoxicity. *Angew. Chem., Int. Ed.* **2015,** *54*, 14383-14387.

(33) Faulkner, A. D.; Kaner, R. A.; Abdallah, Q. M.; Clarkson, G.; Fox, D. J.; Gurnani, P.; Howson, S. E.; Phillips, R. M.; Roper, D. I.; Simpson, D. H.; Scott, P., Asymmetric triplex metallohelices with high and selective activity against cancer cells. *Nat. Chem.* **2014,** *6*, 797-803.

(34) Song, H.; Allison, S. J.; Brabec, V.; Bridgewater, H. E.; Kasparkova, J.; Kostrhunova, H.; Novohradsky, V.; Phillips, R. M.; Pracharova, J.; Rogers, N. J.; Shepherd, S. L.; Scott, P., Glycoconjugated Metallohelices have Improved Nuclear Delivery and Suppress Tumour Growth In Vivo. *Angew. Chem., Int. Ed.* **2020,** *59*, 14677-14685.

(35) Sato, K.; Imai, Y.; Higashi, N.; Kumamoto, Y.; Onami, T. M.; Hedrick, S. M.; Irimura, T., Lack of antigen-specific tissue remodeling in mice deficient in the macrophage galactose-type calcium-type lectin 1/CD301a. *Blood* **2005,** *106*, 207-215.

(36) Ward, S. E.; O'Sullivan, J. M.; Drakeford, C.; Aguila, S.; Jondle, C. N.; Sharma, J.; Fallon, P. G.; Brophy, T. M.; Preston, R. J. S.; Smyth, P.; Sheils, O.; Chion, A.; O'Donnell, J. S., A novel role for the macrophage galactose-type lectin receptor in mediating von Willebrand factor clearance. *Blood* **2018,** *131*, 911-916.

(37) Dusoswa, S. A.; Verhoeff, J.; Abels, E.; Mendez-Huergo, S. P.; Croci, D. O.; Kuijper, L. H.; de Miguel, E.; Wouters, V.; Best, M. G.; Rodriguez, E.; Cornelissen, L. A. M.; van Vliet, S. J.; Wesseling, P.; Breakefield, X. O.; Noske, D. P.; Wurdinger, T.; Broekman, M. L. D.; Rabinovich, G. A.; van Kooyk, Y.; Garcia-Vallejo, J. J., Glioblastomas exploit truncated O-linked glycans for local and distant immune modulation via the macrophage galactose-type lectin. *Proc. Natl. Acad. Sci. U.S.A.* **2020,** *117*, 3693-3703.

(38) Hoober, J. K., ASGR1 and Its Enigmatic Relative, CLEC10A. *Int. J. Mol. Sci.* **2020,** *21*, 4818-4838.

(39) Wu, L.; Zhang, Y.; Li, Z.; Yang, G.; Kochovski, Z.; Chen, G.; Jiang, M., "Sweet" Architecture-Dependent Uptake of Glycocalyx-Mimicking Nanoparticles Based on Biodegradable Aliphatic Polyesters by Macrophages. *J. Am. Chem. Soc.* **2017,** *139*, 14684-14692.

(40) Wei, Z.; Zhang, X.; Yong, T.; Bie, N.; Zhan, G.; Li, X.; Liang, Q.; Li, J.; Yu, J.; Huang, G.; Yan, Y.; Zhang, Z.; Zhang, B.; Gan, L.; Huang, B.; Yang, X., Boosting anti-PD-1 therapy with metformin-loaded macrophage-derived microparticles. *Nat. Commun.* **2021,** *12*, 440.

(41) Khorev, O.; Stokmaier, D.; Schwardt, O.; Cutting, B.; Ernst, B., Trivalent, Gal/GalNAc-containing ligands designed for the asialoglycoprotein receptor. *Bioorg. Med. Chem.* **2008,** *16*, 5216-5231.

(42) Eriksson, M.; Serna, S.; Maglinao, M.; Schlegel, M. K.; Seeberger, P. H.; Reichardt, N. C.; Lepenies, B., Biological evaluation of multivalent lewis X-MGL-1 interactions. *Chembiochem* **2014,** *15*, 844-851.

(43) Andre, S.; O'Sullivan, S.; Koller, C.; Murphy, P. V.; Gabius, H. J., Bi- to tetravalent glycoclusters presenting GlcNAc/GalNAc as inhibitors: from plant agglutinins to human macrophage galactose-type lectin (CD301) and galectins. *Org. Biomol. Chem.* **2015,** *13*, 4190-4203.

(44) Ke, P. C.; Pilkington, E. H.; Sun, Y.; Javed, I.; Kakinen, A.; Peng, G.; Ding, F.; Davis, T. P., Mitigation of Amyloidosis with Nanomaterials. *Adv. Mater.* **2020,** *32*, e1901690.

(45) Du, Z.; Yu, D.; Du, X.; Scott, P.; Ren, J.; Qu, X., Self-triggered click reaction in an Alzheimer's disease model: in situ bifunctional drug synthesis catalyzed by neurotoxic copper accumulated in amyloid-beta plaques. *Chem. Sci.* **2019,** *10*, 10343-10350.

(46) Gao, N.; Du, Z.; Guan, Y.; Dong, K.; Ren, J.; Qu, X., Chirality-Selected Chemical Modulation of Amyloid Aggregation. *J. Am. Chem. Soc.* **2019,** *141*, 6915-6921.

(47) Faridi, A.; Sun, Y.; Okazaki, Y.; Peng, G.; Gao, J.; Kakinen, A.; Faridi, P.; Zhao, M.; Javed, I.; Purcell, A. W.; Davis, T. P.; Lin, S.; Oda, R.; Ding, F.; Ke, P. C., Mitigating Human IAPP Amyloidogenesis In Vivo with Chiral Silica Nanoribbons. *Small* **2018,** *14*, e1802825.

(48) Masters, S. L.; Dunne, A.; Subramanian, S. L.; Hull, R. L.; Tannahill, G. M.; Sharp, F. A.; Becker, C.; Franchi, L.; Yoshihara, E.; Chen, Z.; Mullooly, N.; Mielke, L. A.; Harris, J.; Coll, R. C.; Mills, K. H.; Mok, K. H.; Newsholme, P.; Nunez, G.; Yodoi, J.; Kahn, S. E.; Lavelle,

E. C.; O'Neill, L. A., Activation of the NLRP3 inflammasome by islet amyloid polypeptide provides a mechanism for enhanced IL-1beta in type 2 diabetes. *Nat. Immunol.* **2010,** *11*, 897-904.

(49) Jaiswal, J. K.; Fix, M.; Takano, T.; Nedergaard, M.; Simon, S. M., Resolving vesicle fusion from lysis to monitor calcium-triggered lysosomal exocytosis in astrocytes. *Proc. Natl. Acad. Sci. U.S.A.* **2007,** *104*, 14151-14156.

(50) Aftabizadeh, M.; Tatarek-Nossol, M.; Andreetto, E.; El Bounkari, O.; Kipp, M.; Beyer, C.; Latz, E.; Bernhagen, J.; Kapurniotu, A., Blocking Inflammasome Activation Caused by beta-Amyloid Peptide (Abeta) and Islet Amyloid Polypeptide (IAPP) through an IAPP Mimic. *ACS Chem. Neurosci.* **2019,** *10*, 3703-3717.

(51) Cheng, G.; Li, W.; Ha, L.; Han, X.; Hao, S.; Wan, Y.; Wang, Z.; Dong, F.; Zou, X.; Mao, Y.; Zheng, S. Y., Self-Assembly of Extracellular Vesicle-like Metal-Organic Framework Nanoparticles for Protection and Intracellular Delivery of Biofunctional Proteins. *J. Am. Chem. Soc.* **2018,** *140*, 7282-7291.

(52) Higashi, N.; Fujioka, K.; Denda-Nagai, K.; Hashimoto, S.; Nagai, S.; Sato, T.; Fujita, Y.; Morikawa, A.; Tsuiji, M.; Miyata-Takeuchi, M.; Sano, Y.; Suzuki, N.; Yamamoto, K.; Matsushima, K.; Irimura, T., The macrophage C-type lectin specific for galactose/N-acetylgalactosamine is an endocytic receptor expressed on monocyte-derived immature dendritic cells. *J. Biol. Chem.* **2002,** *277*, 20686-20693.

(53) van Vliet, S. J.; Saeland, E.; van Kooyk, Y., Sweet preferences of MGL: carbohydrate specificity and function. *Trends Immunol.* **2008,** *29*, 83-90.

(54) Bai, N.; Miller, S. A.; Andrianov, G. V.; Yates, M.; Kirubakaran, P.; Karanicolas, J., Rationalizing PROTAC-Mediated Ternary Complex Formation Using Rosetta. *J Chem Inf Model* **2021,** *61*, 1368-1382.

(55) Pierce, B.; Weng, Z., A combination of rescoring and refinement significantly improves protein docking performance. *Proteins* **2008,** *72*, 270-279.

(56) Dong, G. Q.; Fan, H.; Schneidman-Duhovny, D.; Webb, B.; Sali, A., Optimized atomic statistical potentials: assessment of protein interfaces and loops. *Bioinformatics* **2013,** *29*, 3158-3166.

(57) Sanhueza, C. A.; Baksh, M. M.; Thuma, B.; Roy, M. D.; Dutta, S.; Preville, C.; Chrunyk, B. A.; Beaumont, K.; Dullea, R.; Ammirati, M.; Liu, S.; Gebhard, D.; Finley, J. E.; Salatto, C. T.; King-Ahmad, A.; Stock, I.; Atkinson, K.; Reidich, B.; Lin, W.; Kumar, R.; Tu, M.; Menhaji-Klotz, E.; Price, D. A.; Liras, S.; Finn, M. G.; Mascitti, V., Efficient Liver Targeting by Polyvalent Display of a Compact Ligand for the Asialoglycoprotein Receptor. *J. Am. Chem. Soc.* **2017,** *139*, 3528-3536.

(58) Gabba, A.; Bogucka, A.; Luz, J. G.; Diniz, A.; Coelho, H.; Corzana, F.; Canada, F. J.; Marcelo, F.; Murphy, P. V.; Birrane, G., Crystal Structure of the Carbohydrate Recognition Domain of the Human Macrophage Galactose C-Type Lectin Bound to GalNAc and the Tumor-Associated Tn Antigen. *Biochemistry-Us* **2021,** *60*, 1327-1336.

Table of Contents figure